Astronomy-423: Radio Astronomy
Professor: Greg Taylor
Spring 2006

Radio Astronomy Project

VLA and VLBA Observations of AGN

Adam Johnson
Cristina Rodríguez

Introduction

It is important to observe radio sources in order to analyze their astronomical properties. One survey that accomplishes this is The VLBA Imaging and Polarization Survey (VIPS, Taylor et al. 2005). We participated in observing ten radio sources using both the VLA at 5, 8, and 15 GHz and the VLBA at 5 GHz. After the data was calibrated and imaged, analysis ensued. The analysis revealed many interesting properties of the sources which include: the length of jet components, whether polarization is present, size of the core components, spectral index properties, etc.

Observations

VLA

The observations were scheduled by Steve Tremblay and were made in February 2006 on 30 sources at 5, 8, and 15 GHz of which 10 were used in this project. 23 antennas were in operation during the time of observation.

Table 1 lists the ten target sources and the three calibrators used, as well as the time on source for each frequency.

Table 1: Names of the ten target sources and calibrators, as well as the time on source for each frequency

	5 GHz	**8 GHz**	**15 GHz**
Calibrators	Time on source (s)	Time on source (s)	Time on source (s)
1331+305	66.60	62.24	84.88
1407+284	66.31	56.03	114.59
1602+334	79.58	75.14	142.90
Target Sources	Time on source (s)	Time on source (s)	Time on source (s)
J16061+3124	33.44	36.63	36.05
J16074+3528	33.17	35.76	----
J16055+3722	36.05	36.63	36.24
J16083+4012	36.63	36.63	36.34
J16178+3801	36.63	36.63	36.34
J16169+3621	36.34	36.63	36.34
J16235+3559	33.44	36.63	36.34
J16226+3816	33.44	36.34	36.34
J16231+3909	36.63	36.63	36.34
J16325+3547	36.63	36.63	36.34

*Note: Observations were not taken for the source J16074+3528 at 15 GHz

VLBA

The observations were scheduled by Greg Taylor and Joe Helmboldt and were made in December 2005 on 54 sources at 5 GHz of which 10 were used in this project. Table 2 lists the ten target sources as well as the time on source for each frequency.

Table 2: Names of the ten target sources as well as the time on source

Target Sources	Time on source (min)
J16061+3124	108
J16074+3528	112
J16055+3722	121
J16083+4012	127
J16178+3801	120
J16169+3621	119
J16235+3559	128
J16226+3816	119
J16231+3909	127
J16325+3547	122

Calibration

Calibration, self-calibration, and imaging of the VLA data were done using AIPS. Three calibrators were used for flux (1331+305), gain (1602+334), and polarization (1407+284) calibration. The VLBA data was self-calibrated, imaged, and modelfitted using Difmap (calibration was done by Greg Taylor).

Results and Analysis

Redshift and Distances

In order to obtain more information on our sources, we checked the NASA/IPAC Extragalactic Database (NED) web page, and found the position of each source as well as the redshift, a value used to determine the distances. We assumed a value for the Hubble Constant equal to 75 km s^{-1} Mpc^{-1}. There were a few sources for which we did not find the redshift. The classification of the source was also found. All these information is shown in the table below.

Table 3: Type, position, redshift, and distance for the ten target sources and the gain calibrator

Calibrators	Type	RA ; DEC	Redshift	Distance (Mpc)
1602+334	Galaxy	16h02m07.2630s ; +33d26'53.081"	1.10	2521.26
J16061+3124	Galaxy	16h06m08.5159s ; +31d24'46.457"	---	---
J16074+3528	QSO	16h07m24.9876s ; +35d28'00.716"	0.97	2360.9
J16055+3722	QSO	16h05m33.7579s ; +37d22'51.149"	1.798	3093.7
J16083+4012	QSO	16h08m22.1577s ; +40d12'17.828"	0.628	1808.7
J16178+3801	QSO	16h17m48.4068s ; +38d01'41.775"	1.607	2973.8
J16169+3621	QSO	16h16m55.5831s ; +36d21'34.505"	2.264	3313.7
J16235+3559	QSO	16h23m30.5279s ; +35d59'33.138"	0.866	2215.47
J16226+3816	Radio Source	16h22m40.7255s ; +38d16'37.311"	---	---
J16231+3909	QSO	16h23m07.6214s ; +39d09'32.415"	1.975	3187.7
J16325+3547	Radio Source	16h32m31.2544s ; +35d47'37.736"	---	---

VLA

After making final Stokes I images, we measured the rms noise and the peak flux density, and calculated the dynamic range for each of the target sources. Tables 4, 5, and 6 list these figures as well as the expected thermal noise (taken from the VLA calculator) for 5, 8, 15 GHz respectively. These values are also shown for the calibrators 1331+305 and 1602+334.

Table 4: Expected thermal noise, rms noise, peak flux density, and dynamic range at 5 GHz (VLA)

Source	Expected thermal noise (mJy/beam)	rms noise (mJy)	Peak (Jy)	Dynamic range
1331+305	0.1918	0.416	7.370	17726
1602+334	0.1778	0.140	1.580	11270
J16061+3124	0.2740	0.247	0.785	3182
J16074+3528	0.2740	0.198	0.126	637
J16055+3722	0.2740	0.182	0.058	319
J16083+4012	0.2740	0.196	0.151	767
J16178+3801	0.2740	0.171	0.073	426
J16169+3621	0.2740	0.206	0.171	830
J16235+3559	0.2740	0.200	0.166	829
J16226+3816	0.2740	0.169	0.052	311
J16231+3909	0.2740	0.177	0.147	829
J16325+3547	0.2740	0.175	0.266	1516

Table 5: Expected thermal noise, rms noise, peak flux density, and dynamic range at 8 GHz (VLA)

Source	Expected thermal noise (mJy/beam)	rms noise (mJy)	Peak (Jy)	Dynamic range
1331+305	0.170	0.254	5.079	19986
1602+334	0.155	0.090	1.178	13055
J16061+3124	0.222	0.147	0.610	4142
J16074+3528	0.222	0.131	0.115	879
J16055+3722	0.222	0.126	0.062	487
J16083+4012	0.222	0.140	0.177	1263
J16178+3801	0.222	0.132	0.104	785
J16169+3621	0.222	0.131	0.134	1020
J16235+3559	0.222	0.128	0.138	1081
J16226+3816	0.222	0.126	0.055	438
J16231+3909	0.222	0.130	0.101	778
J16325+3547	0.222	0.134	0.172	1282

Table 6: Expected thermal noise, rms noise, peak flux density, and dynamic range at 15 GHz (VLA)

Source	Expected thermal noise (mJy/beam)	rms noise (mJy)	Peak (Jy)	Dynamic range
1331+305	0.527	0.220	3.354	15259
1602+334	0.405	0.263	0.800	3043
J16061+3124	0.808	0.475	0.399	840
J16074+3528*	0.808	---	---	---
J16055+3722	0.808	0.470	0.067	142
J16083+4012	0.808	0.470	0.145	308
J16178+3801	0.808	0.587	0.092	156
J16169+3621	0.808	0.485	0.087	180
J16235+3559	0.808	0.622	0.095	153
J16226+3816	0.808	0.516	0.037	72
J16231+3909	0.808	0.830	0.061	73
J16325+3547	0.808	0.595	0.098	164

*Note: Observations were not taken for the source J16074+3528 at 15 GHz

VLBA

After self-calibrating all the data at 5 GHz, we measured the rms noise, the peak flux density, and the total flux density in the final Stokes I images of the ten target sources, and calculated the dynamic range. The expected thermal noise in this case is 0.36 mJy/beam (value taken from the VLBA calculator). Table 7 lists these figures.

Table 7: Peak flux density, rms noise, dynamic range, and total flux density for the Stokes I images (VLBA)

Source	I peak (Jy)	I rms (mJy)	Dynamic range	I total flux (Jy)
J16061+3124	0.5360	0.440	821	0.738
J16074+3528	0.0970	0.310	3196	0.101
J16055+3722	0.0402	0.339	8433	0.053
J16083+4012	0.1530	0.249	1627	0.150
J16178+3801	0.0690	0.258	3739	0.072
J16169+3621	0.0682	0.217	3182	0.137
J16235+3559	0.0819	0.512	6252	0.122
J16226+3816	0.0390	0.344	8821	0.042
J16231+3909	0.1030	0.280	2716	0.123
J16325+3547	0.1090	0.447	4096	0.242

Comparison Between VLA and VLBA at 5 GHz

The following table shows the ratio between the total flux density measured in the VLBA images and the peak flux density obtained in the VLA images (VLBA/VLA) at 5 GHz for all of our target sources.

Table 8: Ratio between the total flux density in the VLBA images and the peak flux density in the VLA images

5GHz			
Source	**Peak VLA (Jy)**	**Total Flux VLBA (Jy)**	**VLBA/VLA**
J16061+3124	0.785	0.738	0.9406
J16074+3528	0.126	0.101	0.8048
J16055+3722	0.058	0.053	0.9052
J16083+4012	0.151	0.150	0.9967
J16178+3801	0.073	0.072	0.9876
J16169+3621	0.171	0.137	0.7993
J16235+3559	0.166	0.122	0.7373
J16226+3816	0.052	0.042	0.7952
J16231+3909	0.147	0.123	0.8417
J16325+3547	0.266	0.242	0.9090

The VLBA/VLA ratio shows how much flux is recovered in the VLBA image compared to the VLA image. It makes sense these ratios are all less than one, since the VLA has a wider field of view, and thus captures more flux.

Modelfit

In order to calculate sizes as well as the positions of the central and jet components of our sources, elliptical or circular Gaussian components were fitted to the visibility data using Difmap. We found that five of our ten sources show jet components.

Images

Below are the VLBA Stokes I images for all of our target sources, as well as for the calibrator 1602+334. In all of them the contours start at 3σ and are increased by factors of two thereafter. We also show some of the parameters obtained from the modelfit, such as the size of the central component and the length of jets as well as their angle with respect to the central component (all angles measured from north to east).

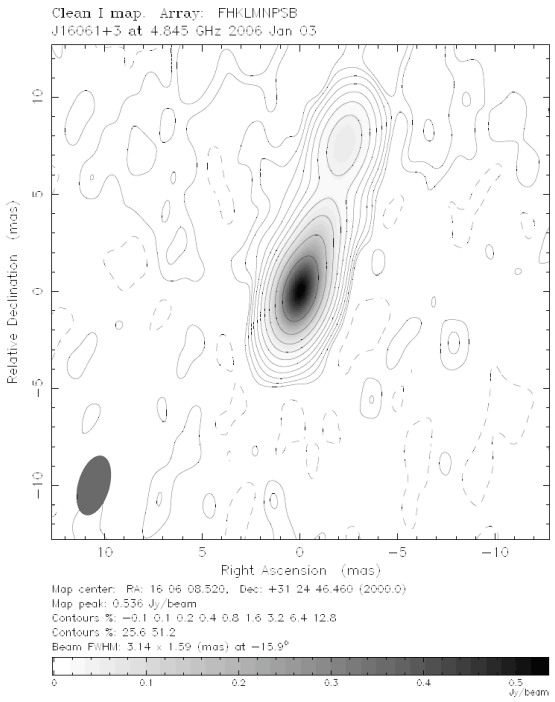

Figure 1. Stokes I image for J16061+3124

- Size of central component: 0.586 mas
- Length of Jet: 7.94 mas
- Jet Angle: 342.4°

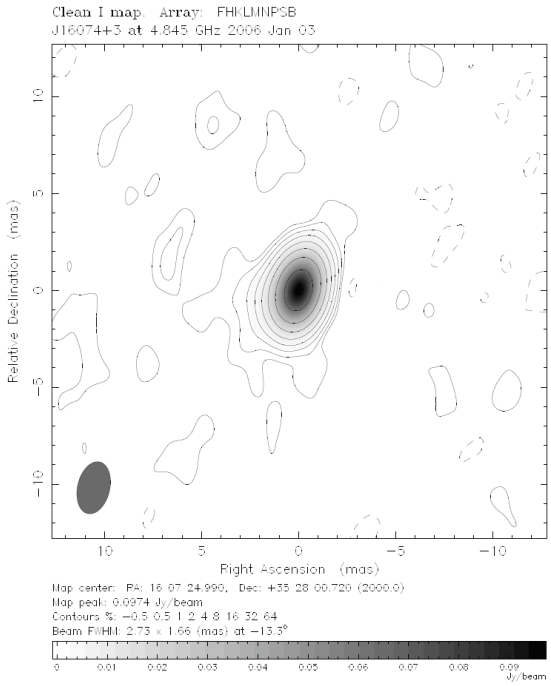

Figure 2. Stokes I image for J16074+3528

- Size of central component: 0.433 mas = 4.96 pc

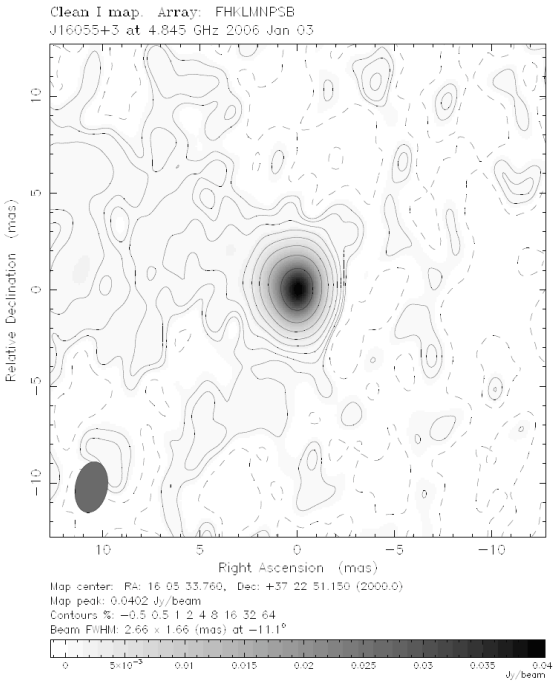

Figure 3. Stokes I image for J16055+3722

- Size of central component: 1.138 mas = 17.01 pc

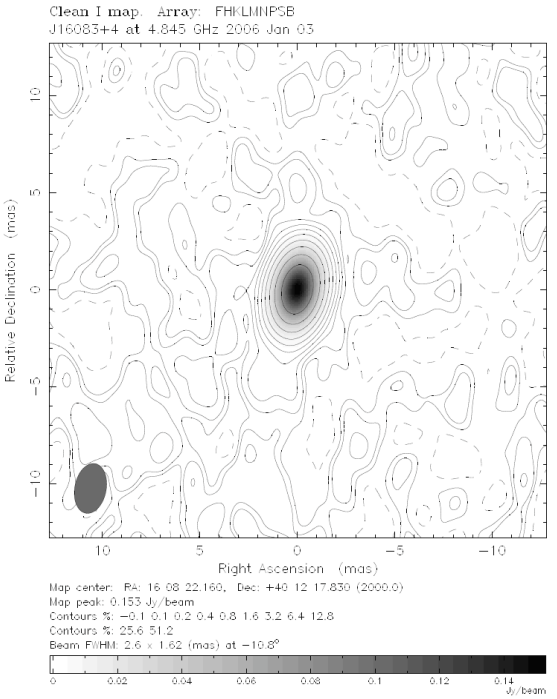

Figure 4. Stokes I image for J16083+4012

Size of central component: 0.023 mas = 0.202 pc

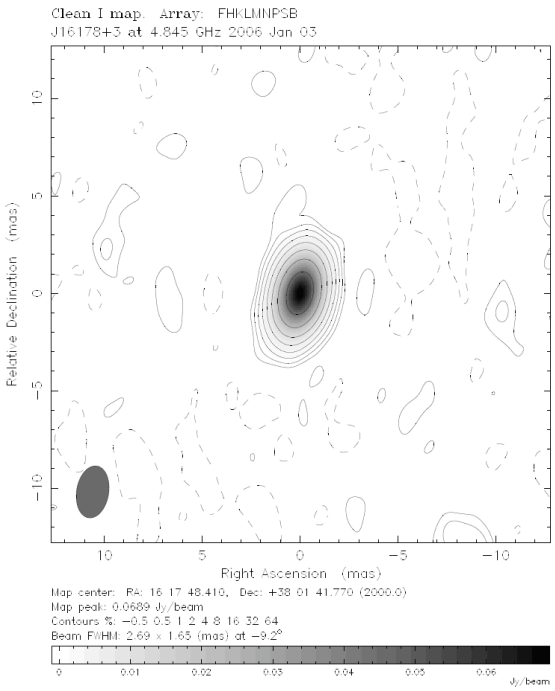

Figure 5. Stokes I image for J16178+3801

Size of central component: 0.339 mas = 4.89 pc

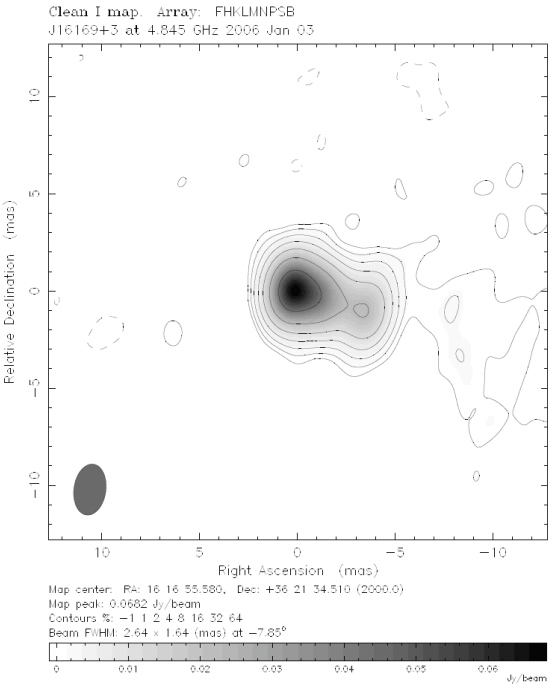

Figure 6. Stokes I image for J16169+3621

- Size of central component: 1.358 mas = 21.83 pc
- Length of Jet: 2.77 mas = 44.52 pc
- Jet Angle: 252.6°

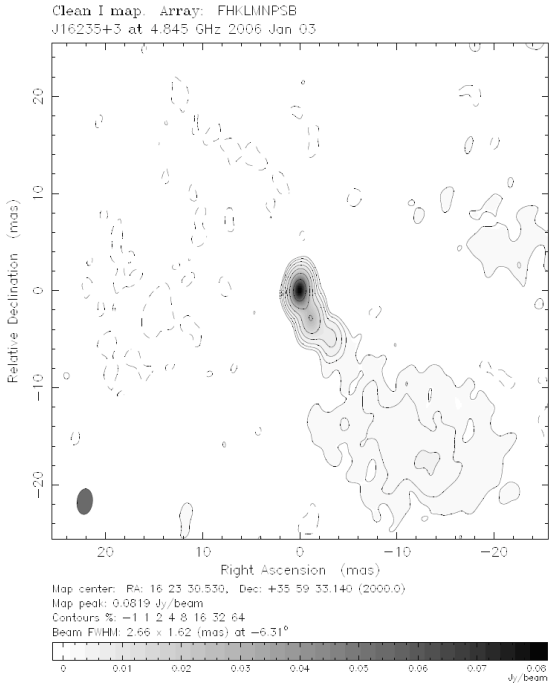

Figure 7. Stokes I image for J16235+3559

-Size of central component: 0.090 mas = 0.97 pc
-Length of Jet: 6.07 mas = 65.22 pc
-Jet Angle: 201.9 °

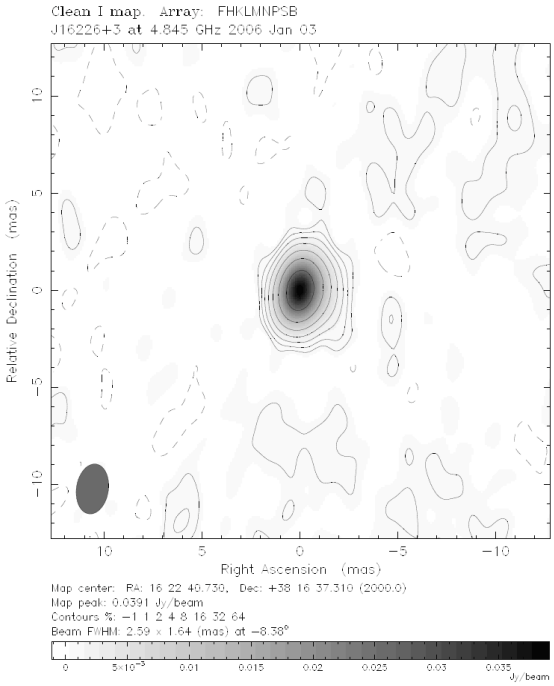

Figure 8. Stokes I image for J16226+3816

- Size of central component: 0.147 mas

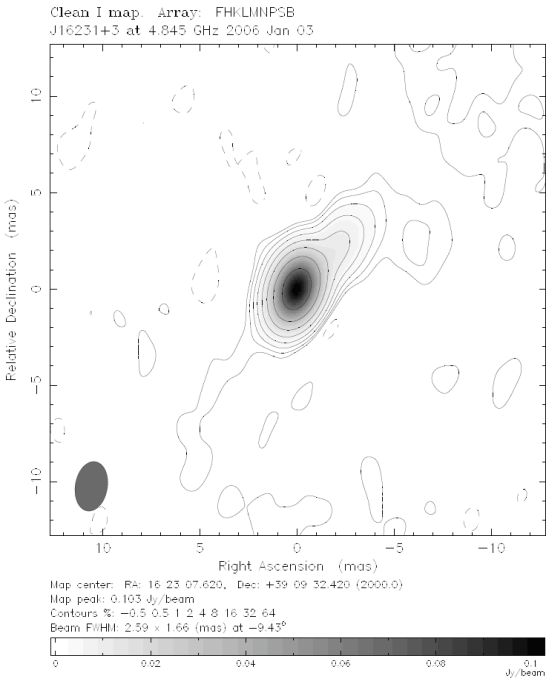

Figure 9. Stokes I image for J16231+3909

- Size of central component: 0.551 mas = 8.52 pc
- Length of Jet: 2.77 mas = 42.83 pc
- Jet Angle: 315.9 °

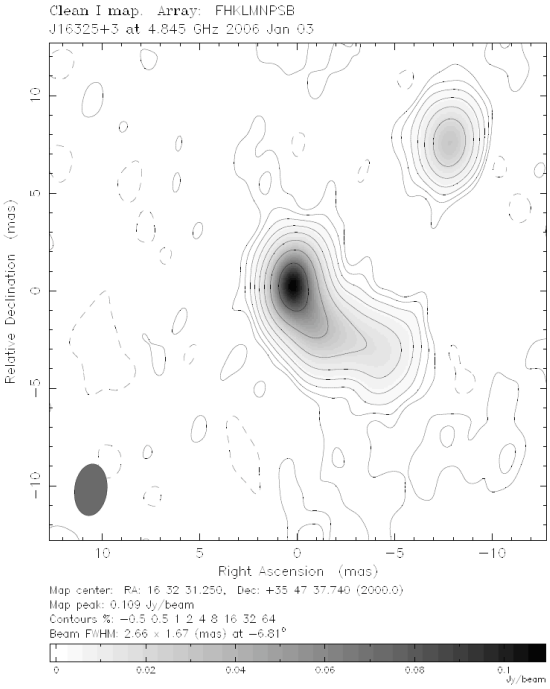

Figure 10. Stokes I image for J16325+3547

- Size of central component: 0.184 mas
- Size of companion: 0.766 mas, 10.88 mas away from central component at 314.2 °
- Length of Jet: 4.08 mas
- Jet Angle: 207.8°

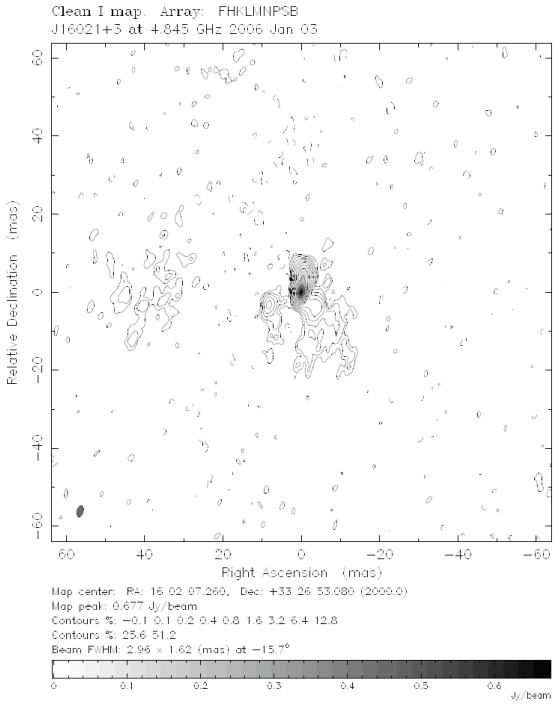

Figure 11. Stokes I image for 1602+334

Spectral Index

Using the values of the peak flux for the VLA data at 5, 8, and 15 GHz, we were able to calculate the spectral indexes $\alpha_{5\text{-}8}$, $\alpha_{8\text{-}15}$, and $\alpha_{5\text{-}15}$ for all of our target sources and the calibrator 1602+334. The results are listed in table 9. We also plotted the peak flux as a function of frequency for all the sources.

Table 9: Spectral index VLA results

Source	$\alpha_{5\text{-}8}$	$\alpha_{8\text{-}15}$	$\alpha_{5\text{-}15}$
J16061+3124	-0.536	-0.676	-0.616
J16074+3528	-0.198		
J16055+3722	0.127	0.134	0.131
J16083+4012	0.336	-0.317	-0.038
J16178+3801	0.753	-0.199	0.208
J16169+3621	-0.518	-0.683	-0.613
J16235+3559	-0.386	-0.591	-0.503
J16226+3816	0.113	-0.632	-0.313
J16231+3909	-0.795	-0.808	-0.803
J16325+3547	-0.924	-0.897	-0.909
1602+334	-0.625	-0.616	-0.619

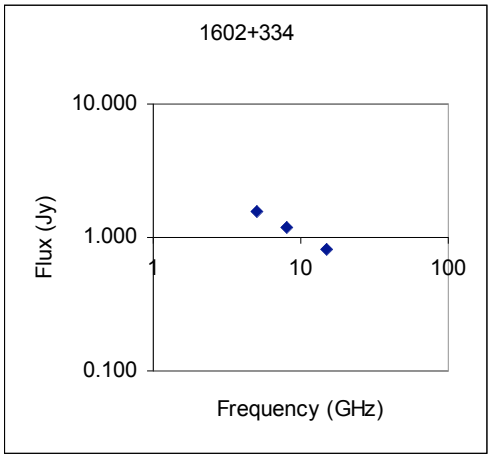
1602+334
10.000
1.000
0.100
Flux (Jy)
1
10
100
Frequency (GHz)

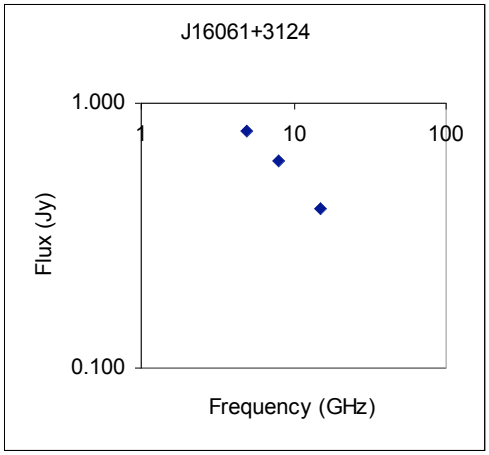
J16061+3124
1.000
0.100
Flux (Jy)
1
10
100
Frequency (GHz)

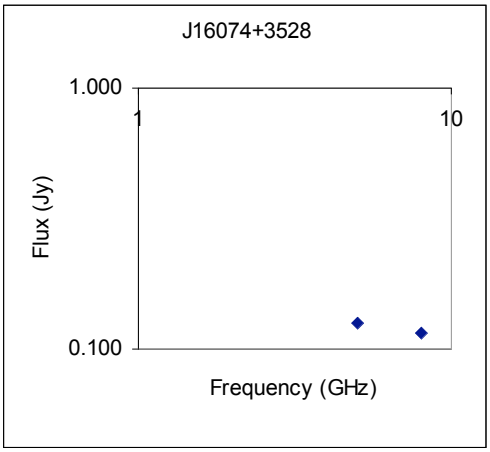
J16074+3528
1.000
0.100
Flux (Jy)
1
10
Frequency (GHz)

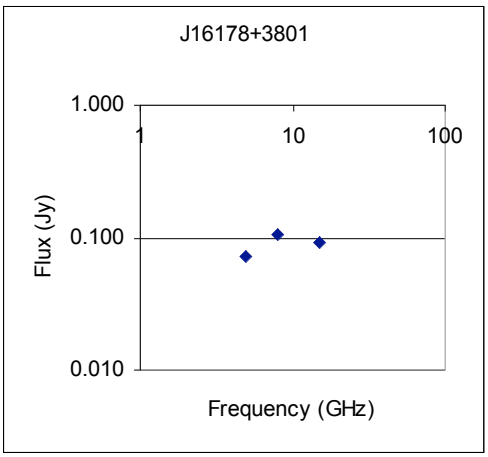
J16178+3801
1.000
0.100
0.010
Flux (Jy)
1
10
100
Frequency (GHz)

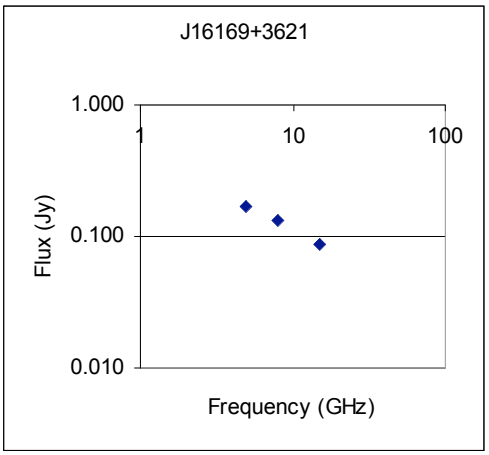
J16169+3621
1.000
0.100
0.010
Flux (Jy)
1
10
100
Frequency (GHz)

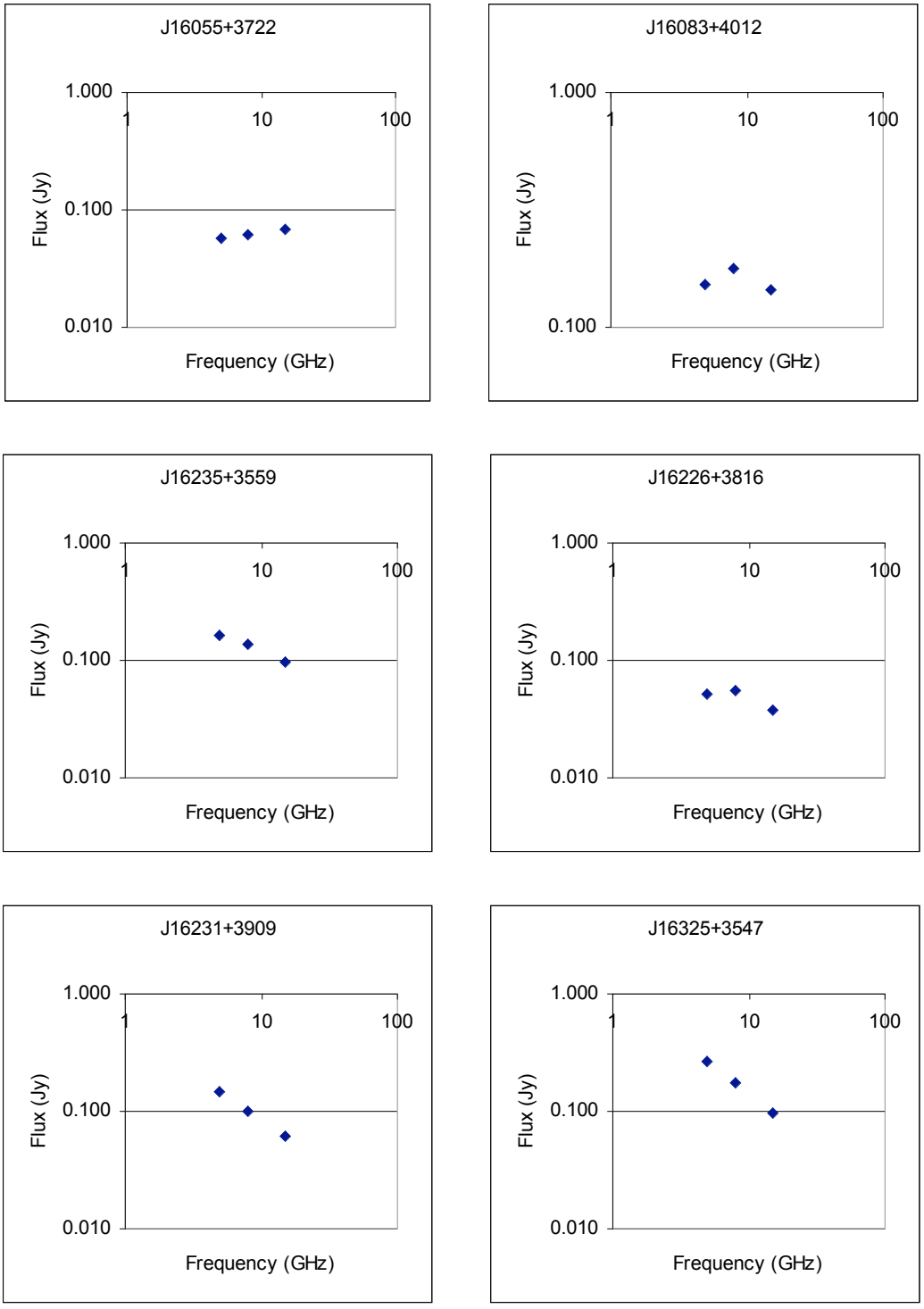

Figure 12. VLA Peak flux density as a function of frequency

From this analysis it can be observed that all the sources presenting a more complex structure showed to have a steep spectrum, while the point sources showed to have either a flat spectrum or a spectrum with a positive slope between 5 and 8 GHz and a negative slope between 8 and 15 GHz, with a peak at around 8 GHz.

The source J16325+3547 show to have an interesting structure. Its steep spectrum shows that the bright central component is likely to be a jet component. In this scenario the northwest

companion is likely to be the core. The central hotspot could be hitting some kind of dense medium, thus changing its direction.

The calibrator 1602+334 also showed some interesting features, which might encourage future study

Polarization Results

In order to determine the polarization angle of our sources we made VLBA Stokes Q and U images in Difmap and then using Aips we measured the integrated peak flux densities using a box centered at the central component. We found two polarized sources out of our ten target sources. The results are listed below.

Table 10: Angle of polarization for the two polarized sources

Source	Peak Q (Jy)	Peak U (Jy)	Angle (deg)
J16055+3722	0.00174	0.0004	5.729
J16169+3621	0.0021594	-0.0005	-6.883

Note: The polarization of J16169+3621 was actually offset from the central component. The Jet showed a polarization angle of -6.9º. The images below were taken off of the VIPS webpage.

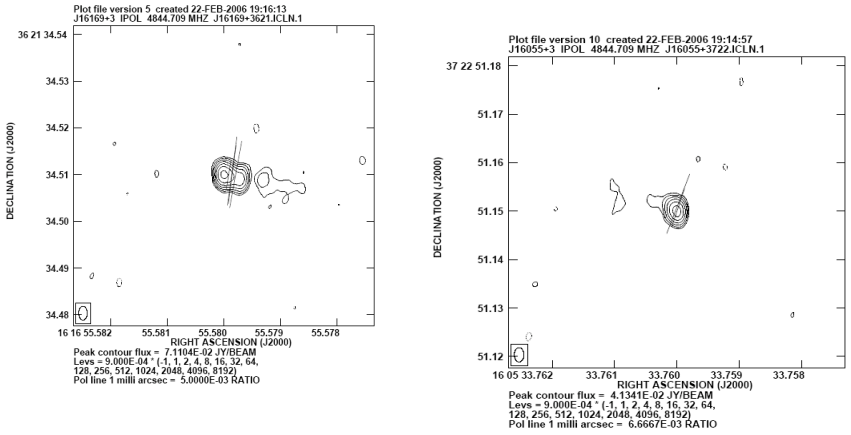

Figure 13. Polarization images obtained from the VIPS webpage for J16055+3722 and J16169+3621

The Stokes Q and U images are shown below.

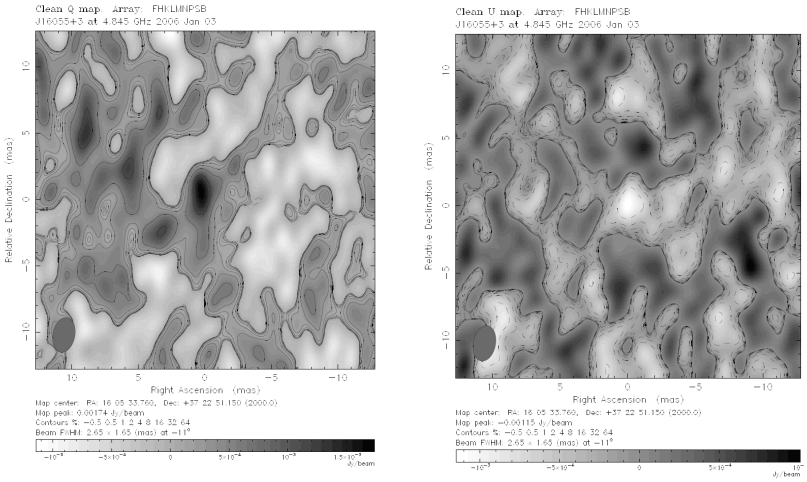

Figure 14. Stokes Q (left) and U (right) images for J16055+3722

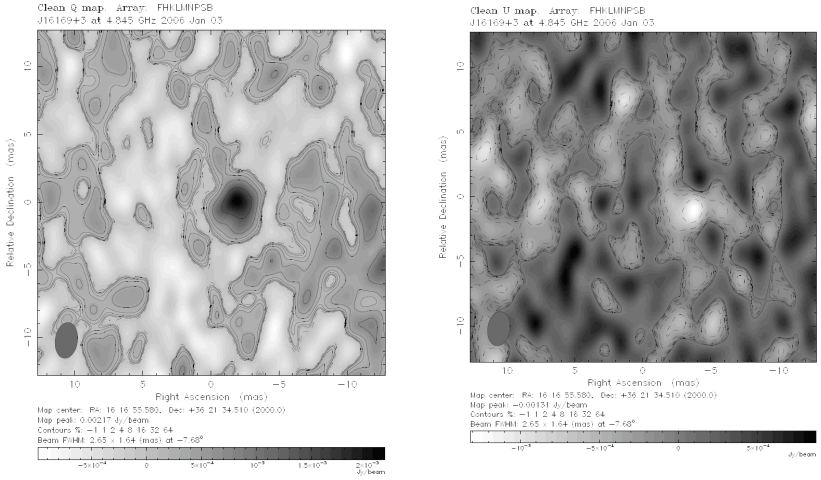

Figure 15. Stokes Q (left) and U (right) images for J16169+3621

Conclusions

Of the ten sources we analyzed, five had jets (50%) and two were polarized (20%). There were several interesting sources, two of which, J16325+3547 and 1602+334 (calibrator), should be considered for future study. Sources that had steep spectrum were found to have more complex structure (such as jets). Though ten radio sources is a small amount of data and not enough to get good statistics, it is a beginning to a large survey that will have in impact on modern astronomy.

References

Taylor, G. b., et al. 2005, ApJS, 159, 27

http://nedwww.ipac.caltech.edu/

http://www.phys.unm.edu/~gbtaylor/VIPS/